

# An Examination of the Relationship between Active Site Loop Size and Thermodynamic Activation Parameters for Orotidine 5'-Monophosphate Decarboxylase from Mesophilic and Thermophilic Organisms<sup>†</sup>

Krisztina Toth,<sup>‡</sup> Tina L. Amyes,<sup>‡</sup> B. McKay Wood,<sup>§</sup> Kui K. Chan,<sup>§</sup> John A. Gerlt,<sup>§</sup> and John P. Richard<sup>\*‡</sup>

<sup>‡</sup>Department of Chemistry, University at Buffalo, SUNY, Buffalo, New York 14260-3000, and <sup>§</sup>Departments of Biochemistry and Chemistry, University of Illinois, Urbana, Illinois 61801

Received June 23, 2009; Revised Manuscript Received July 19, 2009

**ABSTRACT:** Closure of the active site phosphate gripper loop of orotidine 5'-monophosphate decarboxylase from *Saccharomyces cerevisiae* (ScOMPDC) over the bound substrate orotidine 5'-monophosphate (OMP) activates the bound substrate for decarboxylation by at least 10<sup>4</sup>-fold [Amyes, T. L., Richard, J. P., and Tait, J. J. (2005) *J. Am. Chem. Soc.* 127, 15708–15709]. The 19-residue phosphate gripper loop of the mesophilic ScOMPDC is much larger than the nine-residue loop at the ortholog from the thermophile *Methanothermobacter thermautotrophicus* (MtOMPDC). This difference in loop size results in a small decrease in the total intrinsic phosphate binding energy of the phosphodianion group of OMP from 11.9 to 11.6 kcal/mol, along with a modest decrease in the extent of activation by phosphite dianion of decarboxylation of the truncated substrate 1-(β-D-erythrofuransyl)orotic acid. The activation parameters  $\Delta H^\ddagger$  and  $\Delta S^\ddagger$  for  $k_{\text{cat}}$  for decarboxylation of OMP are 3.6 kcal/mol and 10 cal K<sup>-1</sup> mol<sup>-1</sup> more positive, respectively, for MtOMPDC than for ScOMPDC. We suggest that these differences are related to the difference in the size of the active site loops at the mesophilic ScOMPDC and the thermophilic MtOMPDC. The greater enthalpic transition state stabilization available from the more extensive loop–substrate interactions for the ScOMPDC-catalyzed reaction is largely balanced by a larger entropic requirement for immobilization of the larger loop at this enzyme.

Orotidine 5'-monophosphate decarboxylase (OMPDC)<sup>1</sup> is a remarkable enzyme because it employs no metal ions or other cofactors but yet effects an enormous ca. 30 kcal/mol stabilization of the transition state for the chemically very difficult decarboxylation of orotidine 5'-monophosphate (OMP) to give uridine 5'-monophosphate (UMP) (Scheme 1) (1–3). The enormous 10<sup>17</sup>-fold rate acceleration for decarboxylation of enzyme-bound OMP [ $k_{\text{cat}} = 15 \text{ s}^{-1}$  (4)] is a consequence of the exceedingly slow decarboxylation of OMP in water [ $t_{1/2} \approx 78$  million years (3)] through an unstable vinyl carbanion intermediate. This remarkable efficiency led to the proposal of several different mechanisms for the OMPDC-catalyzed reaction that avoid formation of an unstable carbanion (5–10). However, we recently showed that OMPDC meets its catalytic challenge head-on by stabilizing an enzyme-bound vinyl carbanion (Scheme 1) (11, 12).

One of the principal differences between catalysis by enzymes and by small molecules is that enzymes have evolved unique mechanisms to utilize binding interactions with nonreacting portions of the substrate for transition state stabilization (13). We have shown that the binding of phosphite dianion to OMPDC from *Saccharomyces cerevisiae* (yeast, ScOMPDC) results in an 80000-fold increase in the second-order rate constant ( $k_{\text{cat}}/K_{\text{m}}$ ) for enzyme-catalyzed decarboxylation of the truncated substrate 1-(β-D-erythrofuransyl)orotic acid (EO), which lacks a 5'-phosphodianion moiety, to give 1-(β-D-erythrofuransyl)uridine (EU) (Scheme 2) (14). This shows that the nonreacting phosphodianion group of OMP does not function simply to anchor the substrate to the enzyme but rather serves the more important role of activating the enzyme toward decarboxylation of bound OMP.

Similar experiments provided evidence that the “intrinsic phosphate binding energy” of the substrate phosphodianion group of dihydroxyacetone phosphate (DHAP) is utilized in stabilization of the transition state of the aldose–ketose isomerization reaction catalyzed by triosephosphate isomerase (TIM) (15, 16) and of the hydride transfer reaction catalyzed by glycerol-3-phosphate dehydrogenase (GPDH) (Scheme 3) (17).

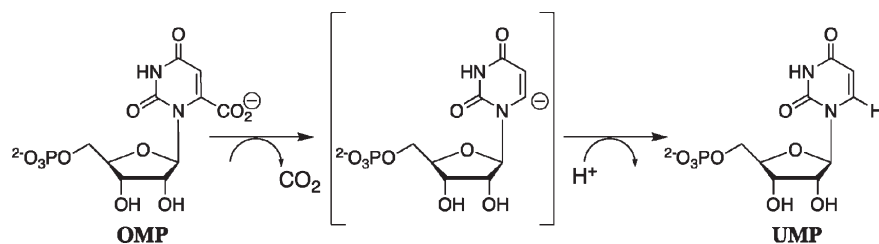
OMPDC (10, 18–22), TIM (23–25), and GPDH (26, 27) each have a flexible “phosphate gripper” loop that is open at the free enzyme but closes over the phosphodianion group of the bound substrate to sequester the substrate from bulk solvent. We have proposed that this phosphate-driven loop closure reduces the barrier for reaction at the loop-closed compared with the loop-open enzymes, and that it is the underlying origin of the

<sup>†</sup>This work was supported by Grants GM39754 to J.P.R. and GM65155 to J.A.G. from the National Institutes of Health.

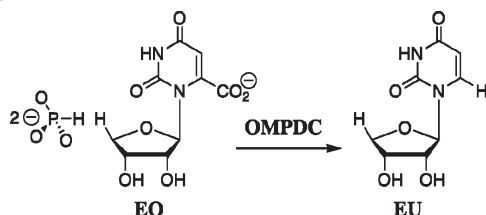
\*To whom correspondence should be addressed. Telephone: (716) 645-4232. Fax: (716) 645-6963. E-mail: jrichard@buffalo.edu.

<sup>1</sup>Abbreviations: OMP, orotidine 5'-monophosphate; UMP, uridine 5'-monophosphate; OMPDC, orotidine 5'-monophosphate decarboxylase; ScOMPDC, orotidine 5'-monophosphate decarboxylase from *Saccharomyces cerevisiae* (yeast); EcOMPDC, orotidine 5'-monophosphate decarboxylase from *Escherichia coli*; MtOMPDC, orotidine 5'-monophosphate decarboxylase from *Methanothermobacter thermautotrophicus*; EO, 1-(β-D-erythrofuransyl)orotic acid; EU, 1-(β-D-erythrofuransyl)uridine; DHAP, dihydroxyacetone phosphate; TIM, triosephosphate isomerase; GPDH, glycerol-3-phosphate dehydrogenase; MOPS, 3-(N-morpholino)propanesulfonic acid; IPTG, isopropyl β-D-thiogalactopyranoside; NADH, nicotinamide adenine dinucleotide, reduced form; PDB, Protein Data Bank.

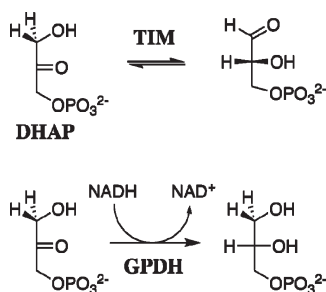
Scheme 1



Scheme 2



Scheme 3



10<sup>4</sup>–10<sup>6</sup>-fold effect of the nonreacting substrate phosphodianion group on the chemical reactivity of the enzyme-bound substrate (17).

The phosphate gripper loops of ScOMPDC and of OMPDC from *Escherichia coli* (EcOMPDC) both extend 19 residues, from the strictly conserved Pro-202 to Val-220 for ScOMPDC (21) (Figure 1) and from Pro-189 to Pro-207 for EcOMPDC (19, 20). By contrast, the corresponding loop of OMPDC from the thermophile *Methanothermobacter thermautotrophicus* (MtOMPDC) extends only nine residues, from Pro-180 to Asp-188 (22) (Figure 1). These three enzymes show an otherwise high degree of structural homology (18) which then raises the question of whether there may be an underlying mechanistic imperative for the difference in the size of the flexible loops for enzymes from mesophiles and thermophiles. For example, if the size of this loop is related to catalytic efficiency, then the smaller loop for MtOMPDC might be expected to play a reduced role in promoting decarboxylation through utilization of the binding energy of the nonreacting substrate phosphodianion group of OMP or of a phosphite dianion activator.

We report here the results of experiments that were designed to compare the intrinsic phosphate binding energy and the thermodynamic activation parameters for OMPDCs from mesophilic and thermophilic organisms. The thermophilic enzyme with the shorter phosphate gripper loop, MtOMPDC, shows an intrinsic phosphate binding energy of the phosphodianion group of OMP and phosphite activation of decarboxylation of the truncated substrate EO that are similar to those observed for the mesophilic ScOMPDC. By contrast, there is a significant difference in the activation parameters  $\Delta H^\ddagger$  and  $\Delta S^\ddagger$  for the decarboxylation of

enzyme-bound OMP such that MtOMPDC pays a substantially smaller entropic price, but a larger enthalpic price, for conversion of the Michaelis complex to the transition state for decarboxylation than ScOMPDC does.

## EXPERIMENTAL PROCEDURES

**Materials.** Orotidine 5'-monophosphate trisodium salt (99%) was purchased from Sigma or was prepared by chemical or enzymatic methods from uridine 5'-monophosphate using modifications of literature procedures (28–30). 1-(β-D-Erythrofuransyl)orotidine (EO) and 1-(β-D-erythrofuransyl)uridine (EU) were available from an earlier study (14). Sodium phosphite (dibasic, pentahydrate), 3-(*N*-morpholino)propanesulfonic acid (MOPS, ≥99.5%), and ammonium acetate (≥99%) were purchased from Fluka. Water was from a Milli-Q Academic purification system. All other chemicals were reagent grade or better and were used without further purification.

**Preparation of OMPDCs.** The C155S mutant OMPDC from *S. cerevisiae* (ScOMPDC) was prepared as described previously (31, 32). This mutant is more stable than, but kinetically and structurally essentially identical with, wild-type yeast OMPDC (33). Wild-type OMPDC from *M. thermautotrophicus* (MtOMPDC) was prepared as described previously (32). The gene for wild-type OMPDC from *E. coli* (EcOMPDC) was cloned from *E. coli* K12 genomic DNA by W. Shan Yew, and the protein was expressed in *E. coli* BL21(DE3) using a modified pET-15b plasmid with a His<sub>10</sub> tag, as described previously for OMPDCs with a His<sub>6</sub> tag (32). The cells were grown at 37 °C, induced with IPTG (0.5 mM) when the cell density reached an OD<sub>600</sub> of 0.6, and harvested after 18 h. Purification was conducted as described previously for ScOMPDC and MtOMPDC (32) except that no Q-Sepharose column was used. The protein was dialyzed at 5 °C against storage buffer [20 mM Tris-HCl (pH 7.0), 100 mM NaCl, and 20% glycerol], concentrated to ca. 25 mg/mL via ultrafiltration, flash-frozen in liquid nitrogen as 25 μL pellets, and stored at –80 °C.

**Preparation of Solutions.** Solution pH was determined at 25 °C using an Orion model 720A pH meter equipped with a Radiometer pHC4006-9 combination electrode that was standardized at pH 7.00 and 10.00 at 25 °C. Stock solutions of OMP were prepared in water, and the OMP concentration was determined from the absorbance in 0.1 M HCl at 267 nm using an  $\epsilon$  of 9430 M<sup>–1</sup> cm<sup>–1</sup> (34). Stock solutions of 1-(β-D-erythrofuransyl)orotidine (EO) were prepared and neutralized to pH ≈ 6 as described previously (14, 31), and the EO concentration was determined from the absorbance in 0.1 M HCl at 267 nm using an  $\epsilon$  of 9570 M<sup>–1</sup> cm<sup>–1</sup> reported for orotidine (34).

The stock solution of phosphite (100 mM, 80% free base, *I* = 0.28) was prepared by addition of a measured amount of 1 M HCl to the sodium salt to give the desired acid/base ratio. MOPS buffers were prepared by addition of measured amounts of 1 M

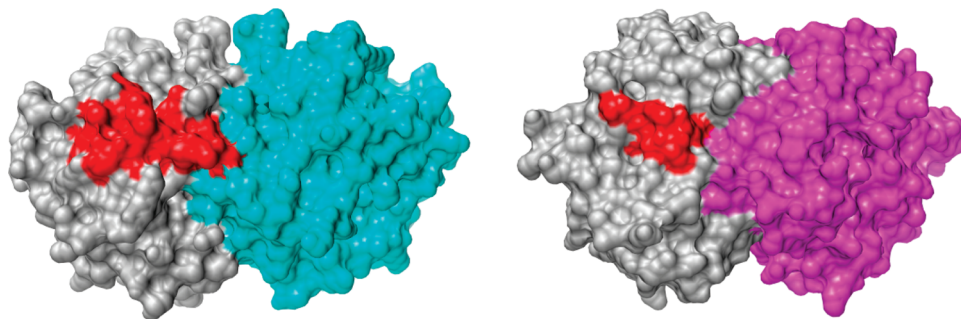


FIGURE 1: Comparison of the closed active site loops of the dimeric OMPDCs from *S. cerevisiae* [19 residues, left structure, PDB entry 3GDL (46)] and *M. thermotrophicus* [nine residues, right structure, PDB entry 3G1A (46)] liganded with 6-azauridine 5'-monophosphate. The active site loops are colored red, and the remainder of the monomer is colored gray. The second monomer is colored cyan (ScOMPDC) or magenta (MtOMPDC). The loop for ScOMPDC extends from Pro-202 to Val-220, and the loop for MtOMPDC extends from Pro-180 to Asp-188. The images were produced using the UCSF Chimera package from the Resource for Biocomputing, Visualization, and Informatics at the University of California, San Francisco (supported by National Institutes of Health Grant P41 RR-01081).

HCl and solid NaCl to give the desired acid/base ratio and ionic strength.

Samples of OMPDCs that had been stored at  $-80^{\circ}\text{C}$  were defrosted and dialyzed at  $4^{\circ}\text{C}$  against 10 mM MOPS (50% free base) (pH 7.1) containing 100 mM NaCl, unless noted otherwise.

**Determination of Values of  $k_{\text{cat}}$  and  $k_{\text{cat}}/K_m$  for Turnover of OMP by OMPDCs at Various Temperatures.** All assays were conducted in 10 mM MOPS (50% free base) at pH 7.1 and  $I = 0.105$  (NaCl) using a Cary 3E spectrophotometer equipped with a temperature-controlled Peltier block multicell changer. The temperature dependence of the difference between the extinction coefficients of OMP and UMP at 279 nm,  $\Delta\epsilon$  ( $\text{M}^{-1}\text{cm}^{-1}$ ), was determined using the following procedure. First, the spectrophotometer was zeroed at 279 nm using a solution of 10 mM MOPS at pH 7.1 and  $I = 0.105$  (NaCl) at  $25^{\circ}\text{C}$ . A small aliquot of OMP was added to give a final concentration of  $100\text{ }\mu\text{M}$  OMP, and the absorbance of the resulting solution was determined at several temperatures between 10 and  $75^{\circ}\text{C}$ . The temperature was then returned to  $25^{\circ}\text{C}$ , and  $1\text{ }\mu\text{L}$  of a solution of ScOMPDC was added to give a final enzyme concentration of 21 nM. The ensuing decarboxylation of OMP was allowed to proceed to completion to give a quantitative yield of UMP, and the final absorbance of the solution was again determined at several temperatures between 10 and  $75^{\circ}\text{C}$ . The observed absorbance changes were used to calculate the following values of  $\Delta\epsilon$  ( $\text{M}^{-1}\text{cm}^{-1}$ ):  $10^{\circ}\text{C}$ , 2290;  $25^{\circ}\text{C}$ , 2400 (4);  $35^{\circ}\text{C}$ , 2490;  $45^{\circ}\text{C}$ , 2560;  $55^{\circ}\text{C}$ , 2610;  $65^{\circ}\text{C}$ , 2660; and  $75^{\circ}\text{C}$ , 2720. The following values of  $\Delta\epsilon$  at other temperatures were obtained by extrapolation or interpolation using the two linear regions of the biphasic linear correlation between  $\Delta\epsilon$  ( $\text{M}^{-1}\text{cm}^{-1}$ ) and  $T$ :  $5^{\circ}\text{C}$ , 2250;  $12^{\circ}\text{C}$ , 2300;  $15^{\circ}\text{C}$ , 2330; and  $17^{\circ}\text{C}$ , 2340.

For the determination of values of  $k_{\text{cat}}$ , the reaction mixtures (1 mL total) containing buffer and OMP ( $[\text{OMP}]_0 = 50\text{--}250\text{ }\mu\text{M}$ ,  $\gg 10K_m$ ) were equilibrated at the temperature of interest and the reaction was initiated by the addition of  $1\text{--}3\text{ }\mu\text{L}$  of a stock solution of OMPDC using a cuvette admixer without removal of the cuvette from the temperature-controlled block. The initial velocity of decarboxylation of OMP under these conditions,  $V_{\text{max}}$  ( $\text{M s}^{-1}$ ), was determined within 1 min by monitoring the decrease in absorbance at 279 nm using the appropriate value of  $\Delta\epsilon$  ( $\text{M}^{-1}\text{cm}^{-1}$ ) for the temperature of interest. The observed values of  $V_{\text{max}}$  were shown to be proportional to enzyme concentration in the following ranges: ScOMPDC, 11–42 nM; MtOMPDC, 76–150 nM; and EcOMPDC, 30–230 nM. At some temperatures, the use of lower concentrations of OMPDC

resulted in reduced activity, presumably as a result of dissociation of the active dimer to give the inactive monomeric form (4). These conditions were 38 nM MtOMPDC at 45 or  $55^{\circ}\text{C}$ , where  $k_{\text{cat}}$  was reduced by 20%; 30 nM EcOMPDC at  $10^{\circ}\text{C}$ , where  $k_{\text{cat}}$  was reduced by 30% (the data were therefore obtained using 60 nM enzyme); 30 nM EcOMPDC at  $5^{\circ}\text{C}$ , where  $k_{\text{cat}}$  was reduced by 50% (the data were therefore obtained using 90–230 nM enzyme); and 15 nM EcOMPDC at  $25^{\circ}\text{C}$ , where  $k_{\text{cat}}$  was reduced by 20%. To verify that the temperature variation did not result in a loss of enzyme activity in the time frame of the assays which were conducted over a period of  $\leq 1$  min (see above), periodic controls were conducted in which the stock solution of OMPDC was incubated in a water bath at the assay temperature of interest for 1–5 min prior to its use in the assay at this temperature. It was found that this preincubation did not significantly affect the observed activity at the temperature of interest.

Values of  $k_{\text{cat}}$  ( $\text{s}^{-1}$ ) were calculated from the values of  $V_{\text{max}}$  ( $\text{M s}^{-1}$ ) using eq 1. In all cases, the concentration of ScOMPDC in the stock solution was calculated from the values of  $V_{\text{max}}$  ( $\text{M s}^{-1}$ ) determined in side-by-side standard assays at  $25^{\circ}\text{C}$  using eq 1 with a  $k_{\text{cat}}$  of  $15\text{ s}^{-1}$  (4). For determination of the values of  $k_{\text{cat}}$  at  $25^{\circ}\text{C}$  for MtOMPDC ( $4.7\text{ s}^{-1}$ ) and EcOMPDC ( $13\text{ s}^{-1}$ ), the concentration of OMPDC was determined from the absorbance of the protein at 280 nm in 10 mM MOPS (50% free base) at pH 7.1 containing 100 mM NaCl and extinction coefficients of  $6100\text{ M}^{-1}\text{cm}^{-1}$  (MtOMPDC) and  $10100\text{ M}^{-1}\text{cm}^{-1}$  (EcOMPDC) that were calculated using the ProtParam tool available on the ExPASy server (35, 36). For determination of the values of  $k_{\text{cat}}$  at other temperatures, the concentrations of MtOMPDC and EcOMPDC were determined from the values of  $V_{\text{max}}$  ( $\text{M s}^{-1}$ ) determined in side-by-side standard assays at  $25^{\circ}\text{C}$  using eq 1 with  $k_{\text{cat}}$  values of 4.7 and  $13\text{ s}^{-1}$ , respectively.

$$k_{\text{cat}} = V_{\text{max}}/[\text{E}] \quad (1)$$

Values of  $k_{\text{cat}}/K_m$  for turnover of OMP by ScOMPDC and MtOMPDC at various temperatures were determined in experiments in which the complete disappearance of a relatively low initial concentration OMP was monitored at 279 nm. Reactions (1 mL total,  $[\text{OMP}]_0 = 4\text{--}40\text{ }\mu\text{M}$ ) were initiated by the addition of OMPDC as described above to give a final concentration of 20–70 nM ScOMPDC or 50–420 nM MtOMPDC. The observed rate constants  $k_{\text{obsd}}$  ( $\text{s}^{-1}$ ) for the first-order decay of OMP in the final stages of the reactions where  $[\text{OMP}]_t \leq 0.3\text{--}0.5K_m$  were obtained from the fits of the absorbance versus time data to a single exponential. Experiments were conducted at



Table 1: Kinetic Parameters and Intrinsic Phosphate Binding Energies for Decarboxylation of OMP and EO Catalyzed by ScOMPDC and MtOMPDC and for the Phosphite-Activated Reactions of EO at pH 7.0 and 25 °C

|         | $k_{\text{cat}}/K_m$ ( $\text{M}^{-1} \text{s}^{-1}$ ) |                       | IPBE <sup>b</sup> (kcal/mol) | $(k_{\text{cat}}/K_m)_{\text{E-HP}}/K_d^c$ ( $\text{M}^{-2} \text{s}^{-1}$ ) | phosphite activation <sup>d</sup> ( $\text{M}^{-1}$ ) |
|---------|--|-----------------------|------------------------------|--|---|
|         | OMP <sup>a</sup>                                       | EO                    |                              |  |   |
| ScOMPDC | $1.1 \times 10^7$                                      | $2.1 \times 10^{-2e}$ | 11.9                         | 11700 <sup>e</sup>   | $5.6 \times 10^5$                                     |
| MtOMPDC | $3.1 \times 10^6$                                      | $8.7 \times 10^{-3}$  | 11.6                         | 2500   | $2.9 \times 10^5$                                     |

<sup>a</sup> Data at pH 7.1 from Table 2. <sup>b</sup> Intrinsic phosphate binding energy calculated from the ratio of the second-order rate constants for the reactions of OMP and EO. <sup>c</sup> Third-order rate constant for phosphite-activated decarboxylation of EO catalyzed by OMPDC, calculated as the slope of the plot of  $(k_{\text{cat}}/K_m)_{\text{obsd}}$  vs  $[\text{HPO}_3^{2-}]$  at low concentrations of phosphite (Figure 2). <sup>d</sup> Ratio of the third-order rate constant for the phosphite-activated decarboxylation of EO and the second-order rate constant for the unactivated decarboxylation of EO. <sup>e</sup> Data at pH 7.1 from ref 14.

several enzyme concentrations in the indicated ranges to ensure that the observed first-order decay represents enzyme-catalyzed reaction of OMP rather than a loss of enzyme activity with time, and the values of  $k_{\text{obsd}}$  were shown to be proportional to  $[\text{E}]$ . Values of  $k_{\text{cat}}/K_m$  ( $\text{M}^{-1} \text{s}^{-1}$ ) were then calculated using the relationship  $k_{\text{cat}}/K_m = k_{\text{obsd}}/[\text{E}]$ , and values of  $K_m$  for OMP were obtained by combining the experimental values of  $k_{\text{cat}}$  ( $\text{s}^{-1}$ ) and  $k_{\text{cat}}/K_m$  ( $\text{M}^{-1} \text{s}^{-1}$ ) (see Table 1). In all cases, the concentration of OMPDC was determined from the values of  $V_{\text{max}}$  ( $\text{M s}^{-1}$ ) determined in side-by-side standard assays at 25 °C using eq 1 with the appropriate value of  $k_{\text{cat}}$ . This analysis is possible because the initial concentration of OMP in these experiments ( $[\text{OMP}]_0 \leq 40 \mu\text{M}$ ) was chosen (see below) such that the amount of the UMP product generated ( $\leq 40 \mu\text{M}$ ) is insufficient to result in significant inhibition of the OMPDC of interest. The initial concentration of OMP ( $[\text{OMP}]_0$ ) was chosen on the basis of the following: For ScOMPDC, a  $K_i$  value of  $400 \mu\text{M}$  has been reported for binding of UMP to ScOMPDC at 25 °C under our experimental conditions (4), and there was no significant change in the value of  $K_m$  determined in our experiments at 45 °C for an  $[\text{OMP}]_0$  of 11–33  $\mu\text{M}$ . For MtOMPDC at 25 °C, experiments conducted at an  $[\text{OMP}]_0$  of 200–400  $\mu\text{M}$  yielded apparent values of  $K_m$  that are consistent with values of  $K_i$  for binding of UMP to MtOMPDC of ca. 100  $\mu\text{M}$  at 25 °C and ca. 200  $\mu\text{M}$  at 55 °C. There was no significant change in the value of  $K_m$  determined in our experiments when the initial concentration of OMP was varied in the range of 6–30  $\mu\text{M}$  at 5 °C, 4–12  $\mu\text{M}$  at 25 °C, 12–22  $\mu\text{M}$  at 35 °C, or 18–39  $\mu\text{M}$  at 55 °C.

**Turnover of EO by MtOMPDC in the Absence and Presence of Phosphite Dianion.** The decarboxylation of the truncated substrate 1-( $\beta$ -D-erythrofuransyl)orotic acid (EO, 5 mM) in 50 mM MOPS (45% free base) at pH 7.0, 25 °C, and  $I = 0.14$  (NaCl) catalyzed by MtOMPDC (350  $\mu\text{M}$ ) was followed in a discontinuous assay in which the initial velocity of formation of the product 1-( $\beta$ -D-erythrofuransyl)uridine (EU) was monitored by HPLC. For these experiments, MtOMPDC was dialyzed at 4 °C against 100 mM MOPS (45% free base) at pH 7.0 and  $I = 0.28$  (NaCl). The reaction in a total volume of 200  $\mu\text{L}$  was initiated by the addition of EO to a solution of the enzyme in buffer that was equilibrated at 25 °C. The reaction was followed for ca. 7 h, during which time there was 8% reaction of EO. At various times, an aliquot (20  $\mu\text{L}$ ) was withdrawn and quenched to pH 3.8 by the addition of 180  $\mu\text{L}$  of ice-cold 5 mM formic acid. The enzyme was removed by ultrafiltration using an Amicon Microcon filtration device (10K molecular weight cutoff), and the filtrate (150  $\mu\text{L}$ ) was analyzed by HPLC using a using a Waters Atlantis dC<sub>18</sub> 3  $\mu\text{m}$  column (3.9 mm  $\times$  150 mm) with an isocratic flow of 10 mM NH<sub>4</sub>OAc (pH 4.2) at a rate of 1 mL/min and peak detection at 262 nm. Under these conditions, the unreacted EO eluted close to the void volume and the product

EU eluted at ca. 7 min. The concentration of the product EU in the reaction mixture at time  $t$ ,  $[\text{EU}]_t$ , was obtained from the HPLC peak area by interpolation of a standard curve that was constructed using authentic EU. The concentration of MtOMPDC in the reaction mixture was determined by a periodic standard assay (see above), and it was shown that there was no significant decrease in enzyme activity during the reaction. The initial velocity of the reaction,  $v_i$  ( $\text{M s}^{-1}$ ), was determined as the slope of the linear plot of  $[\text{EU}]_t$  versus time. The second-order rate constant,  $(k_{\text{cat}}/K_m)_0$  ( $\text{M}^{-1} \text{s}^{-1}$ ), for MtOMPDC-catalyzed decarboxylation of EO was calculated using the relationship  $(k_{\text{cat}}/K_m)_0 = v_i/[\text{E}][\text{S}]_0$ .

The decarboxylation of EO (0.12 mM) in the presence of 2–36 mM phosphite dianion and 5 mM MOPS at pH 7.0, 25 °C, and  $I = 0.14$  (NaCl) catalyzed by MtOMPDC (22–38  $\mu\text{M}$ ) was monitored spectrophotometrically at 283 nm. Reactions (1 mL total volume) were initiated by the addition of 50  $\mu\text{L}$  of a solution of MtOMPDC in 100 mM MOPS [pH 7.0 and  $I = 0.28$  (NaCl)] and were monitored for up to 6 h. The concentration of MtOMPDC in the reaction mixture was determined by a standard assay, and it was shown that there was no significant decrease in enzyme activity during the reaction. These reactions obeyed excellent first-order kinetics with stable end points, and values of  $k_{\text{obsd}}$  ( $\text{s}^{-1}$ ) for the reaction of EO were obtained from the fits of the absorbance versus time data to a single exponential. The apparent second-order rate constants,  $(k_{\text{cat}}/K_m)_{\text{obsd}}$  ( $\text{M}^{-1} \text{s}^{-1}$ ), for MtOMPDC-catalyzed decarboxylation of EO at the various concentrations of phosphite dianion were calculated using the relationship  $(k_{\text{cat}}/K_m)_{\text{obsd}} = k_{\text{obsd}}/[\text{E}]$ .

## RESULTS

The second-order rate constant for decarboxylation of the truncated substrate 1-( $\beta$ -D-erythrofuransyl)orotic acid (EO) lacking a 5'-phosphodianion group catalyzed by OMPDC from *M. thermotrophicus* (MtOMPDC) at pH 7.0, 25 °C, and  $I = 0.14$  (NaCl) was determined as  $(k_{\text{cat}}/K_m)_0 = 8.7 \times 10^{-3} \text{ M}^{-1} \text{s}^{-1}$  (Table 1).

Figure 2 shows the dependence of the apparent second-order rate constant  $(k_{\text{cat}}/K_m)_{\text{obsd}}$  for decarboxylation of the truncated substrate EO catalyzed by MtOMPDC on the concentration of added phosphite dianion at pH 7.0, 25 °C, and  $I = 0.14$  (NaCl). There is no evidence for saturation of MtOMPDC by phosphite dianion, and the data for  $< 30 \text{ mM HPO}_3^{2-}$  show a good fit to eq 2 that was derived for the mechanism shown in Scheme 4 where  $[\text{HPO}_3^{2-}] \ll K_d$ . The slope of the correlation gives a value for the third-order rate constant for the phosphite-activated reaction  $[(k_{\text{cat}}/K_m)_{\text{E-HP}}/K_d]$  of  $2500 \text{ M}^{-2} \text{s}^{-1}$  (Table 1). However, there are small (ca. 30%) positive deviations of the data at 36 mM  $\text{HPO}_3^{2-}$  from the linear correlation established for

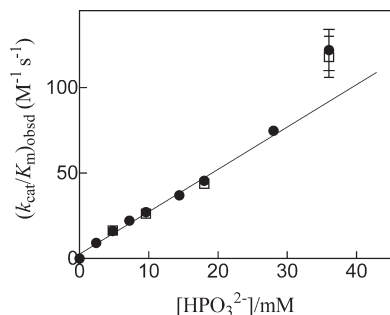
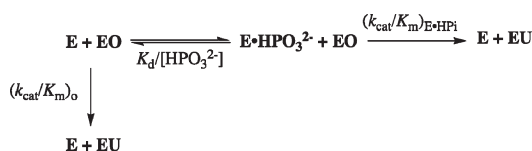


FIGURE 2: Dependence of  $(k_{\text{cat}}/K_m)_{\text{obsd}}$  for the decarboxylation of EO catalyzed by MtOMPDC on the concentration of added phosphite dianion at pH 7.0, 25 °C, and  $I = 0.14$  (NaCl). The filled and empty symbols represent data obtained in two independent experiments that were reproducible to within 5%. The slope of the correlation gives the third-order rate constant  $[(k_{\text{cat}}/K_m)/K_d = 2500 \text{ M}^{-1} \text{ s}^{-1}]$  for the phosphite-activated reaction. The data at 36 mM  $\text{HPO}_3^{2-}$  include error bars that indicate the estimated maximum range of experimental error ( $\pm 10\%$ ), and they were not included in the correlation (see the text).

Scheme 4



< 30 mM  $\text{HPO}_3^{2-}$  (Figure 2). A control experiment at 18 mM  $\text{HPO}_3^{2-}$ , 12 mM  $\text{Cl}^-$ , and 63 mM  $\text{NO}_3^-$  ( $I = 0.14$ ) gave a  $(k_{\text{cat}}/K_m)_{\text{obsd}}$  value of  $6.3 \text{ M}^{-1} \text{ s}^{-1}$ , which is 7-fold lower than the corresponding value of  $46 \text{ M}^{-1} \text{ s}^{-1}$  determined at 18 mM  $\text{HPO}_3^{2-}$  and 75 mM  $\text{Cl}^-$  ( $I = 0.14$ ). This suggests that there are specific salt effects on the activity of MtOMPDC associated with the replacement of chloride with other anions.

$$(k_{\text{cat}}/K_m)_{\text{obsd}} = (k_{\text{cat}}/K_m)_o + \frac{(k_{\text{cat}}/K_m)_{\text{E} \cdot \text{HPi}} [\text{HPO}_3^{2-}]}{K_d} \quad (2)$$

Table 2 reports the kinetic parameters  $k_{\text{cat}}$ ,  $k_{\text{cat}}/K_m$ , and  $K_m$  for decarboxylation of OMP catalyzed by ScOMPDC, MtOMPDC, and EcOMPDC at various temperatures between 5 and 55 °C. Care was taken to work at concentrations of OMPDC at which the enzyme exists mainly in the active dimeric form (4). It was routinely shown that the kinetic parameters are independent of the concentration of both OMPDC and the initial concentration of OMP used for their determination. Control experiments were conducted to ensure that the temperature variation did not result in a loss of enzyme activity in the time frame of the assays.

## DISCUSSION

A comparison of the kinetic parameters for decarboxylation of the whole substrate OMP and the truncated substrate EO (Table 1) shows that the binding interactions between the enzyme and the 5'-phosphodianion group of OMP are responsible for the  $5.2 \times 10^8$ - and  $3.6 \times 10^8$ -fold increases, respectively, in the second-order rate constant for decarboxylation of the truncated substrate EO catalyzed by ScOMPDC and MtOMPDC. These rate increases correspond to intrinsic phosphate binding energies of 11.9 and 11.6 kcal/mol, respectively (14). These results are consistent with a somewhat larger transition state stabilization from interactions of the phosphodianion group of the enzyme-bound ligand with the long flexible phosphate gripper

loop of the mesophilic ScOMPDC (19 residues) compared with the shorter flexible loop of the thermophilic MtOMPDC (nine residues) (Figure 1).

We have reported intrinsic phosphate binding energies of 12.2 and  $\geq 11.0$  kcal/mol for the deprotonation of (*R*)-glyceraldehyde 3-phosphate catalyzed by TIM (16) and the reduction of DHAP by NADH catalyzed by GPDH (17), respectively, each of which has a phosphate gripper loop that results in optimal interaction of the substrate phosphodianion group with the protein catalyst (23–27). The similarity in the intrinsic phosphate binding energies for three enzymes that catalyze a variety of chemical reactions suggests that 12 kcal/mol serves as the effective upper limit on the intrinsic phosphate binding energy obtained after billions of years of evolutionary pressure to select for optimal protein catalysts of these different reactions. We suggest that phosphate gripper loops are essential for obtaining this large intrinsic phosphate binding energy, because they provide the protein with the means to make a maximal number of contacts with the substrate, which binds initially at an open active site cleft and then becomes buried in the protein interior upon loop closure (13, 37).

We reported earlier that the binding of phosphite dianion to ScOMPDC strongly activates the enzyme toward decarboxylation of the truncated substrate EO lacking a 5'-phosphodianion group (14). Figure 2 shows that phosphite dianion is also a potent activator of the decarboxylation of EO catalyzed by MtOMPDC. The ratio of the third-order rate constant,  $(k_{\text{cat}}/K_m)_{\text{E} \cdot \text{HPi}}/K_d$  (Scheme 4), for the phosphite-activated decarboxylation of EO and the second-order rate constant,  $(k_{\text{cat}}/K_m)_o$ , for the unactivated decarboxylation of EO provides a good measure of the extent of activation by subsaturating concentrations of phosphite dianion. Values of the  $[(k_{\text{cat}}/K_m)_{\text{E} \cdot \text{HPi}}/K_d]/(k_{\text{cat}}/K_m)_o$  ratios of  $5.6 \times 10^5$  and  $2.9 \times 10^5 \text{ M}^{-1}$  for the reactions catalyzed by ScOMPDC and MtOMPDC, respectively (Table 1), show that the larger flexible phosphate gripper loop at the enzyme from yeast results in a slightly larger advantage from phosphite activation. We conclude that the large reduction in loop size for the thermophilic compared with mesophilic enzyme does not have a severe effect on either phosphodianion activation of the whole OMP or phosphite dianion activation of the truncated substrate EO.

**Temperature Dependence of  $k_{\text{cat}}$  for OMPDCs from Various Organisms.** Figure 3 shows Eyring plots of  $k_{\text{cat}}$  for decarboxylation of OMP catalyzed by ScOMPDC, MtOMPDC, and EcOMPDC over the temperature range of 5–55 °C (278–328 K) according to eq 3. Table 3 gives the derived values of  $\Delta H^\ddagger$  and  $\Delta S^\ddagger$  that were calculated from the slopes ( $-\Delta H^\ddagger/R$ ) and intercepts ( $\Delta S^\ddagger/R$ ) of these correlations, respectively. The activation parameters for ScOMPDC and EcOMPDC are very similar so that there is almost no change in the relative values of  $k_{\text{cat}}$  for these enzymes with a change in temperature. However, the ratio of the values of  $k_{\text{cat}}$  for ScOMPDC and MtOMPDC decreases from 4.8 at 5 °C to 1.9 at 45 °C, which reflects the larger value of  $\Delta H^\ddagger$  for MtOMPDC [14.8 kcal/mol (Table 3)] than for ScOMPDC (11.2 kcal/mol). These results show that, compared with ScOMPDC, MtOMPDC makes better use of the greater thermal energy that is available at the higher temperature maximum for this thermophilic enzyme.

$$\ln(k_{\text{cat}}h/k_B T) = \frac{\Delta S^\ddagger}{R} - \frac{\Delta H^\ddagger}{RT} \quad (3)$$

The entropy of activation for MtOMPDC [ $-6.0 \text{ cal K}^{-1} \text{ mol}^{-1}$  (Table 3)] is more positive than for ScOMPDC ( $-16 \text{ cal K}^{-1} \text{ mol}^{-1}$ ),

Table 2: Temperature Dependence of the Kinetic Parameters for Decarboxylation of OMP Catalyzed by ScOMPDC, MtOMPDC, and EcOMPDC at pH 7.1 and  $I = 0.1$  (NaCl)<sup>a</sup>

| temp (°C) | ScOMPDC                               |   |              | MtOMPDC                               |   |              | EcOMPDC                               |
|-----------|---------------------------------------|---|--------------|---------------------------------------|---|--------------|---------------------------------------|
|           | $k_{\text{cat}}^b$ (s <sup>-1</sup> ) | $k_{\text{cat}}/K_m^c$ (M <sup>-1</sup> s <sup>-1</sup> ) | $K_m^d$ (μM) | $k_{\text{cat}}^b$ (s <sup>-1</sup> ) | $k_{\text{cat}}/K_m^c$ (M <sup>-1</sup> s <sup>-1</sup> ) | $K_m^d$ (μM) | $k_{\text{cat}}^b$ (s <sup>-1</sup> ) |
| 5         | 3.1 ± 0.5                             | (2.7 ± 0.2) × 10 <sup>6</sup>                             | 1.1 ± 0.2    | 0.64 ± 0.03                           | (6.0 ± 2.2) × 10 <sup>5</sup>                             | 1.1 ± 0.4    | 2.5 ± 0.1                             |
| 10        | 4.6 ± 0.6                             | (3.2 ± 0.2) × 10 <sup>6</sup>                             | 1.4 ± 0.2    |                                       |   |              | 3.7 ± 0.1                             |
| 12        | 5.1 ± 0.5                             |   |              |                                       |   |              |                                       |
| 15        | 6.9 ± 0.9                             | (5.6 ± 0.4) × 10 <sup>6</sup>                             | 1.2 ± 0.2    | 2.0 ± 0.3                             | (1.4 ± 0.2) × 10 <sup>6</sup>                             | 1.5 ± 0.3    | 6.4 ± 0.1                             |
| 17        | 7.8 ± 0.8                             |   |              |                                       |   |              |                                       |
| 25        | 15 ± 1                                | (1.1 ± 0.1) × 10 <sup>7</sup>                             | 1.4 ± 0.2    | 4.7 ± 0.3                             | (3.1 ± 0.3) × 10 <sup>6</sup>                             | 1.5 ± 0.2    | 13 ± 1                                |
| 35        | 27 ± 1                                | (1.7 ± 0.4) × 10 <sup>7</sup>                             | 1.6 ± 0.4    | 11 ± 1                                | (4.2 ± 0.9) × 10 <sup>6</sup>                             | 2.8 ± 0.6    | 23 ± 1                                |
| 45        | 45 ± 4                                | (1.4 ± 0.2) × 10 <sup>7</sup>                             | 3.3 ± 0.6    | 24 ± 2                                | (5.0 ± 1.3) × 10 <sup>6</sup>                             | 4.8 ± 1.4    | 35 ± 1                                |
| 50        | 59 ± 6                                | (7.5 ± 0.3) × 10 <sup>6</sup>                             | 7.9 ± 0.9    |                                       |   |              |                                       |
| 55        |                                       |   |              | 44 ± 2                                | (6.1 ± 0.9) × 10 <sup>6</sup>                             | 7.3 ± 1.1    |                                       |

<sup>a</sup> The quoted errors in  $k_{\text{cat}}$  and  $k_{\text{cat}}/K_m$  are standard errors that were obtained from multiple experiments to determine these parameters. <sup>b</sup> Determined from the initial velocity of decarboxylation of OMP when  $[\text{OMP}]_0 \geq 20K_m$ . The observed values of  $k_{\text{cat}}$  were independent of enzyme concentration in the range of 11–42 nM for ScOMPDC, 76–152 nM for MtOMPDC, and 30–230 nM for EcOMPDC (see the text). <sup>c</sup> Determined from the first-order rate constant for decarboxylation of OMP ( $[\text{OMP}]_0 \leq 40 \mu\text{M}$ ) when  $[\text{OMP}]_i = 0.3\text{--}0.5K_m$  (see the text). <sup>d</sup> Calculated from the values of  $k_{\text{cat}}$  and  $k_{\text{cat}}/K_m$ . The standard error was obtained by propagation of the standard errors in  $k_{\text{cat}}$  and  $k_{\text{cat}}/K_m$ .

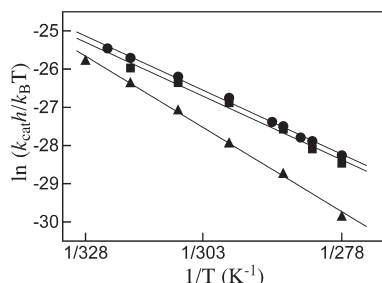


FIGURE 3: Temperature dependence of  $k_{\text{cat}}$  (s<sup>-1</sup>) for the decarboxylation of saturating OMP catalyzed by OMPDCs from various organisms plotted according to the Eyring equation (eq 3): (●) ScOMPDC, (■) EcOMPDC, and (▲) MtOMPDC.

so that there is a larger unfavorable enthalpic and smaller unfavorable entropic change for conversion of the ground state Michaelis complex to the transition state for MtOMPDC-catalyzed decarboxylation than for the ScOMPDC-catalyzed reaction. We suggest that the difference in the size of the active site loops at MtOMPDC and ScOMPDC results in the observed difference in the activation parameters for these enzymes. The greater enthalpic transition state stabilization may reflect the more extensive loop–substrate interactions for the ScOMPDC-catalyzed reaction, and these are suggested to be balanced by a greater entropic requirement for immobilization of the larger loop at the ES complex and transition state for the yeast enzyme. A similar difference in the enthalpy and entropy of activation has been observed for the mesophilic lactate dehydrogenase from *Deinococcus radiourans* and the corresponding thermophilic enzyme from *Thermus thermophilus* where the role of loops in catalysis is less well-defined (47).

For many enzymes, it has been shown that increases in protein thermostability are often the result of enhanced networks of stabilizing ionic interactions between the side chains of amino acid residues (38). These added ionic interactions have the effect of restricting protein conformational changes, so that at the same temperature, enzymes from thermophiles are often more rigid than their mesophilic counterparts (39, 40). For example, a study of neutron scattering by the thermophilic malate dehydrogenase from *Methanococcus jannaschii* and a mesophilic analogue, lactate dehydrogenase from *Oryzotagus cuniculus* (rabbit muscle), shows that the root-mean-square fluctuations (1.5 Å) are similar for these enzymes at the temperature of their optimal activity (41).

Table 3: Activation Parameters for  $k_{\text{cat}}$  for Decarboxylation of OMP Catalyzed by OMPDCs from *S. cerevisiae*, *E. coli*, and *M. thermotrophicus*<sup>a</sup>

| enzyme  | $\Delta H^\ddagger$ (kcal/mol) <sup>b</sup> | $\Delta S^\ddagger$ (cal K <sup>-1</sup> mol <sup>-1</sup> ) <sup>c</sup> |
|---------|---|---|
| ScOMPDC | 11.2  | −16   |
| EcOMPDC | 11.2  | −16   |
| MtOMPDC | 14.8  | −6.0  |

<sup>a</sup> For reactions at pH 7.1 and  $I = 0.1$  (NaCl) (data from Table 2). Activation parameters were determined from Eyring plots covering the range of 278–328 K [5–55 °C (Figure 3)]. <sup>b</sup> Determined from the slopes of the correlations in Figure 3 according to eq 3. <sup>c</sup> Determined from the intercepts of the correlations in Figure 3 according to eq 3.

The similar conformational flexibility observed for enzymes at their temperature optima suggests that the restriction of protein motions below a threshold level might cripple catalytic activity (40, 42, 43). Similarly, loop movement is required both to trap OMPDC-bound substrate (loop closure) and to release the product (loop opening), yet the loop must remain fixed as the loop-closed enzyme–substrate complex is converted to product.

We suggest that efficient substrate binding and catalysis require both flexibility of the loop to allow for efficient transport of the ligand to and from OMPDC and rigidity at the closed ES and ES<sup>‡</sup> complexes. Truncation of the large flexible phosphate gripper loop for the mesophilic enzyme on moving to the thermophilic MtOMPDC might maintain this balance by reducing the degree of high-temperature motion of the loop when it is closed over the substrate. This would have the additional effect of weakening the stabilizing interactions between the loop and the substrate phosphodianion group, thereby leading to an increase in  $\Delta H^\ddagger$  and a decrease in the kinetic parameters for the reaction catalyzed by the thermophilic enzyme at 25 °C (Figure 3). However, the increase in  $\Delta H^\ddagger$  also sharpens the temperature dependence for the thermophilic enzyme-catalyzed reaction and helps to ensure that the thermophilic and mesophilic enzymes have similar kinetic parameters at their respective operating temperatures.

*Effects of Temperature on  $k_{\text{cat}}/K_m$  for OMPDCs from Various Organisms.* Figure 4 shows the effect of changing temperature on  $k_{\text{cat}}/K_m$  for decarboxylation of OMP catalyzed by ScOMPDC and MtOMPDC. For both enzymes, roughly linear correlations of  $\ln(k_{\text{cat}}/K_m)$  with  $1/T$  are observed at low



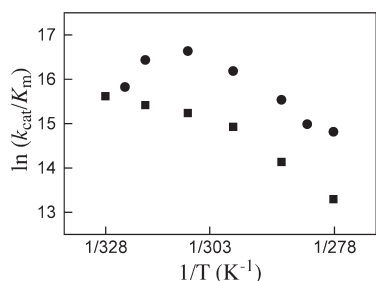


FIGURE 4: Correlations of  $\ln(k_{\text{cat}}/K_m)$  with  $1/T$  for the decarboxylation of a subsaturating amount of OMP catalyzed by ScOMPDC (●) and MtOMPDC (■).

temperatures ( $<35^\circ\text{C}$ , 308 K), where the value of  $K_m$  is essentially constant and the overall change in  $k_{\text{cat}}/K_m$  is due to the increase in  $k_{\text{cat}}$  with the increase in  $T$  (Table 2). For ScOMPDC, there is a sharp downward break in the correlation at  $35^\circ\text{C}$  (308 K), where  $k_{\text{cat}}/K_m$  ( $1.7 \times 10^7 \text{ M}^{-1} \text{ s}^{-1}$ ) reaches a maximum (Table 2). This downward break reflects the sharp increases in the Michaelis constant  $K_m$  with an increasing temperature, which outweigh the increases in  $k_{\text{cat}}$ . These observations are consistent with a change in the rate-determining step for  $k_{\text{cat}}/K_m$  for ScOMPDC from rate-determining decarboxylation ( $k_{\text{cat}}, k_{-1} > k_{\text{cat}}$ , eq 4) for reactions at low temperatures to rate-determining substrate binding ( $k_1, k_{-1} < k_{\text{cat}}$ , eq 4) for reactions at higher temperatures (Scheme 5) (44, 45). The fractional dependence of  $k_{\text{cat}}/K_m$  on solvent viscosity (32) and the experimental rate constant ratio ( $k_{-1}/k_{\text{cat}}$ ) of  $\approx 4$  (4) determined for ScOMPDC-catalyzed decarboxylation of OMP at  $25^\circ\text{C}$  show that substrate binding ( $k_1$ ) is already partly rate-determining at this temperature. Therefore, if the temperature dependence of  $k_{-1}$  for breakdown of the E•OMP complex is small, a change in the rate-determining step with an increase in temperature should be observed (Scheme 5).

$$k_{\text{cat}}/K_m = \frac{k_1 k_{\text{cat}}}{k_{-1} + k_{\text{cat}}} \quad (4)$$

For MtOMPDC, the downward break in the correlation in Figure 4 at  $25^\circ\text{C}$  (298 K) where  $k_{\text{cat}}/K_m = 3.1 \times 10^6 \text{ M}^{-1} \text{ s}^{-1}$  is probably due to a similar change in the rate-determining step for the reaction of OMP. The difference in the limiting  $k_{\text{cat}}/K_m$  values of  $6.1 \times 10^6 \text{ M}^{-1} \text{ s}^{-1}$  [ $T = 55^\circ\text{C}$  (Table 2)] and  $1.7 \times 10^7 \text{ M}^{-1} \text{ s}^{-1}$  [ $T = 35^\circ\text{C}$  (Table 2)] for the reactions catalyzed by MtOMPDC and ScOMPDC, respectively, suggests that simple diffusion of substrate to the enzyme active sites cannot be rate-determining for both reactions. We suggest that the barrier to loop reorganization to “trap” the substrate at the enzyme active site contributes to the activation barriers for formation of an encounter complex, and that this former barrier is larger for the MtOMPDC-catalyzed reaction.

**Conclusions and Speculation.** A large positive  $\Delta H^\ddagger$  allows thermophilic enzymes to make efficient use of the large thermal heat energy available from their environment by maximizing the increase in reactivity as the temperature is increased. A small negative  $\Delta S^\ddagger$  will minimize unfavorable temperature effects associated with an increase in “order” on proceeding from the enzyme–substrate complex to the transition state. We suggest that these thermodynamic constraints favor the evolution of truncated flexible active site loops at enzymes from thermophilic organisms. The results reported here support the conclusion that the relatively short flexible phosphate gripper loop at OMPDC

## Scheme 5



from the thermophile *M. thermautotrophicus* provides a smaller enthalpic transition state stabilization, but that this enthalpic stabilization carries a lower entropic price, compared with the transition state stabilization provided by the larger loops at OMPDCs from the mesophiles *S. cerevisiae* and *E. coli*. This tentative conclusion is not meant to minimize the possible relevance and contribution of other protein motions to the activation barriers for enzyme-catalyzed reactions.

## REFERENCES

- Callahan, B. P., and Miller, B. G. (2007) OMP decarboxylase: An enigma persists. *Bioorg. Chem.* 35, 465–469.
- Miller, B. G., and Wolfenden, R. (2002) Catalytic proficiency: The unusual case of OMP decarboxylase. *Annu. Rev. Biochem.* 71, 847–885.
- Radzicka, A., and Wolfenden, R. (1995) A proficient enzyme. *Science* 267, 90–93.
- Porter, D. J. T., and Short, S. A. (2000) Yeast Orotidine-5'-Phosphate Decarboxylase: Steady-State and Pre-Steady-State Analysis of the Kinetic Mechanism of Substrate Decarboxylation. *Biochemistry* 39, 11788–11800.
- Stanton, C. L., Kuo, I. F., Mundy, C. J., Laino, T., and Houk, K. N. (2007) QM/MM metadynamics study of the direct decarboxylation mechanism for orotidine-5'-monophosphate decarboxylase using two different QM regions: Acceleration too small to explain rate of enzyme catalysis. *J. Phys. Chem. B* 111, 12573–12581.
- Silverman, R., and Groziak, M. (1982) Model chemistry for a covalent mechanism of action of orotidine 5'-phosphate decarboxylase. *J. Am. Chem. Soc.* 104, 6434–6439.
- Shostak, K., and Jones, M. E. (1992) Orotidylate decarboxylase: Insights into the catalytic mechanism from substrate specificity studies. *Biochemistry* 31, 12155–12161.
- Lee, J. K., and Houk, K. N. (1997) A proficient enzyme revisited: The predicted mechanism for orotidine monophosphate decarboxylase. *Science* 276, 942–945.
- Lee, T.-S., Chong, L. T., Chodera, J. D., and Kollman, P. A. (2001) An alternative explanation for the catalytic proficiency of orotidine 5'-phosphate decarboxylase. *J. Am. Chem. Soc.* 123, 12837–12848.
- Appleby, T. C., Kinsland, C., Begley, T. P., and Ealick, S. E. (2000) The crystal structure and mechanism of orotidine 5'-monophosphate decarboxylase. *Proc. Natl. Acad. Sci. U.S.A.* 97, 2005–2010.
- Toth, K., Amyes, T. L., Wood, B. M., Chan, K., Gerlt, J. A., and Richard, J. P. (2007) Product Deuterium Isotope Effect for Orotidine 5'-Monophosphate Decarboxylase: Evidence for the Existence of a Short-Lived Carbanion Intermediate. *J. Am. Chem. Soc.* 129, 12946–12947.
- Amyes, T. L., Wood, B. M., Chan, K., Gerlt, J. A., and Richard, J. P. (2008) Formation and Stability of a Vinyl Carbanion at the Active Site of Orotidine 5'-Monophosphate Decarboxylase:  $pK_a$  of the C-6 Proton of Enzyme-Bound UMP. *J. Am. Chem. Soc.* 130, 1574–1575.
- Jencks, W. P. (1975) Binding energy, specificity, and enzymic catalysis: The Circe effect. *Adv. Enzymol. Relat. Areas Mol. Biol.* 43, 219–410.
- Amyes, T. L., Richard, J. P., and Tait, J. J. (2005) Activation of orotidine 5'-monophosphate decarboxylase by phosphite dianion: The whole substrate is the sum of two parts. *J. Am. Chem. Soc.* 127, 15708–15709.
- Amyes, T. L., and Richard, J. P. (2007) Enzymatic catalysis of proton transfer at carbon: Activation of triosephosphate isomerase by phosphite dianion. *Biochemistry* 46, 5841–5854.
- Amyes, T. L., O'Donoghue, A. C., and Richard, J. P. (2001) Contribution of phosphate intrinsic binding energy to the enzymatic rate acceleration for triosephosphate isomerase. *J. Am. Chem. Soc.* 123, 11325–11326.
- Tsang, W.-Y., Amyes, T. L., and Richard, J. P. (2008) A Substrate in Pieces: Allosteric Activation of Glycerol 3-Phosphate Dehydrogenase ( $\text{NAD}^+$ ) by Phosphite Dianion. *Biochemistry* 47, 4575–4582.
- Begley, T. P., and Ealick, S. E. (2004) Enzymatic reactions involving novel mechanisms of carbanion stabilization. *Curr. Opin. Chem. Biol.* 8, 508–515.

19. Harris, P., Poulsen, J.-C. N., Jensen, K. F., and Larsen, S. (2000) Structural basis for the catalytic mechanism of a proficient enzyme: Orotidine 5'-monophosphate decarboxylase. *Biochemistry* 39, 4217–4224.
20. Harris, P., Poulsen, J. C., Jensen, K. F., and Larsen, S. (2002) Substrate binding induces domain movements in orotidine 5'-monophosphate decarboxylase. *J. Mol. Biol.* 318, 1019–1029.
21. Miller, B. G., Hassell, A. M., Wolfenden, R., Milburn, M. V., and Short, S. A. (2000) Anatomy of a proficient enzyme: The structure of orotidine 5'-monophosphate decarboxylase in the presence and absence of a potential transition state analog. *Proc. Natl. Acad. Sci. U.S.A.* 97, 2011–2016.
22. Wu, N., Mo, Y., Gao, J., and Pai, E. F. (2000) Electrostatic stress in catalysis: Structure and mechanism of the enzyme orotidine monophosphate decarboxylase. *Proc. Natl. Acad. Sci. U.S.A.* 97, 2017–2022.
23. Sampson, N. S., and Knowles, J. R. (1992) Segmental movement: Definition of the structural requirements for loop closure in catalysis by triosephosphate isomerase. *Biochemistry* 31, 8482–8487.
24. Sampson, N. S., and Knowles, J. R. (1992) Segmental motion in catalysis: Investigation of a hydrogen bond critical for loop closure in the reaction of triosephosphate isomerase. *Biochemistry* 31, 8488–8494.
25. Pompliano, D. L., Peyman, A., and Knowles, J. R. (1990) Stabilization of a reaction intermediate as a catalytic device: definition of the functional role of the flexible loop in triosephosphate isomerase. *Biochemistry* 29, 3186–3194.
26. Ou, X., Ji, C., Han, X., Zhao, X., Li, X., Mao, Y., Wong, L.-L., Bartlam, M., and Rao, Z. (2006) Crystal structures of human glycerol 3-phosphate dehydrogenase 1 (GPD1). *J. Mol. Biol.* 357, 858–869.
27. Suresh, S., Turley, S., Oppendoor, F. R., Michels, P. A. M., and Hol, W. G. H. (2000) A potential target enzyme for trypanocidal drugs revealed by the crystal structure of NAD-dependent glycerol-3-phosphate dehydrogenase from *Leishmania mexicana*. *Structure* 8, 541–552.
28. Smiley, J. A., Paneth, P., O'Leary, M. H., Bell, J. B., and Jones, M. E. (1991) Investigation of the enzymic mechanism of yeast orotidine-5'-monophosphate decarboxylase using carbon-13 kinetic isotope effects. *Biochemistry* 30, 6216–6223.
29. Miller, B. G., Butterfoss, G. L., Short, S. A., and Wolfenden, R. (2001) Role of Enzyme-Ribofuranosyl Contacts in the Ground State and Transition State for Orotidine 5'-Phosphate Decarboxylase: A Role for Substrate Destabilization? *Biochemistry* 40, 6227–6232.
30. Van Vleet, J. L., Reinhardt, L. A., Miller, B. G., Sievers, A., and Cleland, W. W. (2008) Carbon isotope effect study on orotidine 5'-monophosphate decarboxylase: Support for an anionic intermediate. *Biochemistry* 47, 798–803.
31. Barnett, S. A., Amyes, T. L., Wood, B. M., Gerlt, J. A., and Richard, J. P. (2008) Dissecting the Total Transition State Stabilization Provided by Amino Acid Side Chains at Orotidine 5'-Monophosphate Decarboxylase: A Two-Part Substrate Approach. *Biochemistry* 47, 7785–7787.
32. Wood, B. M., Chan, K. K., Amyes, T. L., Richard, J. P., and Gerlt, J. A. (2009) Mechanism of the Orotidine 5'-Monophosphate Decarboxylase-Catalyzed Reaction: Effect of Solvent Viscosity on Kinetic Constants. *Biochemistry* 48, 5510–5517.
33. Sievers, A., and Wolfenden, R. (2005) The effective molarity of the substrate phosphoryl group in the transition state for yeast OMP decarboxylase. *Bioorg. Chem.* 33, 45–52.
34. Moffatt, J. G. (1963) The synthesis of orotidine 5'-phosphate. *J. Am. Chem. Soc.* 85, 1118–1123.
35. Gasteiger, E., Gattiker, A., Hoogland, C., Ivanyi, I., Appel, R. D., and Bairoch, A. (2003) ExPASy: The proteomics server for in-depth protein knowledge and analysis. *Nucleic Acids Res.* 31, 3784–3788.
36. Gasteiger, E., Hoogland, C., Gattiker, A., Duvaud, S., Wilkins, M. R., Appel, R. D., and Bairoch, A. (2005) in *Proteomics Protocols Handbook* (Walker, J. M., Ed.) pp 571–607, Humana Press Inc., Totowa, NJ.
37. Herschlag, D. (1988) The role of induced fit and conformational changes of enzymes in specificity and catalysis. *Bioorg. Chem.* 16, 62–96.
38. Vielle, C., and Zeikus, G. J. (2001) Hyperthermophilic Enzymes: Sources, Uses, and Molecular Mechanisms for Thermostability. *Microbiol. Mol. Biol. Rev.* 65, 1–43.
39. Wrba, A., Schweiger, A., Schultes, V., Jaenicke, R., and Zavodszky, P. (1990) Extremely thermostable D-glyceraldehyde-3-phosphate dehydrogenase from the eubacterium *Thermotoga maritima*. *Biochemistry* 29, 7584–7592.
40. Zavodszky, P., Kardos, J., Svingor, Á., and Petsko, G. A. (1998) Adjustment of conformational flexibility is a key event in the thermal adaptation of proteins. *Proc. Natl. Acad. Sci. U.S.A.* 95, 7406–7411.
41. Tehei, M. (2005) Neutron Scattering Reveals the Dynamic Basis of Protein Adaptation to Extreme Temperature. *J. Biol. Chem.* 280, 40974–40979.
42. Liang, Z., Lee, T., Resing, K. A., Ahn, N. G., and Klinman, J. (2004) Thermal-activated protein mobility and its correlation with catalysis in thermophilic alcohol dehydrogenase. *Proc. Natl. Acad. Sci. U.S.A.* 101, 9556–9561.
43. Liang, Z.-X., Tsigos, I., Bouriotis, V., and Klinman, J. P. (2004) Impact of Protein Flexibility on Hydride-Transfer Parameters in Thermophilic and Psychrophilic Alcohol Dehydrogenases. *J. Am. Chem. Soc.* 126, 9500–9501.
44. Brouwer, A., and Kirsch, J. (1982) Investigation of diffusion-limited rates of chymotrypsin reactions by viscosity variation. *Biochemistry* 21, 1302–1307.
45. Lim, W., Raines, R., and Knowles, J. (1988) Triosephosphate isomerase catalysis is diffusion controlled. Appendix: Analysis of triose phosphate equilibria in aqueous solution by phosphorus-31 NMR. *Biochemistry* 27, 1165–1167.
46. Chan, K. K., Wood, B. M., Fedorov, A. A., Fedorov, E. V., Imker, H. J., Amyes, T. L., Richard, J. P., Almo, S. C., and Gerlt, J. A. (2009) Mechanism of the Orotidine 5'-Monophosphate Decarboxylase-Catalyzed Reaction: Evidence for Substrate Destabilization. *Biochemistry* 48, 5518–5531.
47. Coquelle, N., Fioravanti, E., Weik, M., Vellieux, F., and Madern, D. (2007) Activity, Stability and Structural Studies of Lactate Dehydrogenases Adapted to Extreme Thermal Environments. *J. Mol. Biol.* 374, 547–562.